

An Analysis of Mechanical Properties and Flexural Behavior of Concrete Slabs Reinforced with H.F.R.P Reinforcements: A Review

Prerna Vaidya, Prof. Nitesh Kushwaha, Prof. Afzal Khan

Department of Civil Engineering, Millennium Institute of Technology, Bhopal, Madhya Pradesh, India

ABSTRACT

In the era of concrete, concrete is exposed to chemical, such as carbonation and chloride adulteration break down the alkaline barrier in the cement. Subsequently, steel in the concrete becomes corrosive. Such phenomena lead to erosion of concrete at the reinforcement level, cracking and spelling of concrete due to volume increase of steel reinforcement. Different methods were investigated to overcome corrosion by numerous researchers.

According to A.S.T.M D792-13 standards the density of H.F.R.P bars have been evaluated the experimental value with 0.1mg precision. As per the standards, the H.F.R.P bars are weighed. Then, the H.F.R.P bar is immersed in distilled water at 230C and the wet weight of the bar is noted. The weight of the Sinker in immersed condition is also noted.

The laboratory tests carried out to evaluate the physical and mechanical properties of the newly developed H.F.R.P bars and are compared with that of conventional bars. The bond properties of H.F.R.P bars with concrete is also determined. Finally, it explains the experimental investigations on the flexural behavior of concrete one-way slabs reinforced with H.F.R.P reinforcements under static loading and are compared with conventional ones. The stress-strain performance of the sand-coated H.F.R.P bar is linear, lacking yield point up to the failure transverse shear strength is 3 times lesser than the tensile strength of the H.F.R.P bars. Thermal properties of fibers are substantially different in the longitudinal and transverse direction. Therefore the thermal characteristics vary between products according to the fiber, matrix and the fiber volume ratio. In this study the longitudinal Coefficient of linear thermal expansion is

$7.5 \times 10^{-6}/^{\circ}\text{C}$ to $9 \times 10^{-6}/^{\circ}\text{C}$. Whereas the transverse Coefficient of linear thermal expansion is between $15 \times 10^{-6}/^{\circ}\text{C}$ to $20 \times 10^{-6}/^{\circ}\text{C}$. Load -deflection graphs drawn exhibits the accordance between experimental and FEM (ANSYS) observations. The reduced deflection of FEM is due to the rigidness of meshing. The results also confer about the effect of tension stiffening and the bond slip. From the comparison it has been observed that experimental deflections vary from 1.03 to 1.37 times higher than the FEM deflections.

KEYWORDS: H.F.R.P, Transverse Shear Strength, Flexural Behavior, FEM, Bond Properties, Compressive Strength

1. INTRODUCTION

1.1. GENERAL

In the era of concrete, concrete is exposed to chemical, such as carbonation and chloride adulteration break down the alkaline barrier in the cement. Subsequently, steel in the concrete becomes corrosive. Such phenomena lead to erosion of concrete at the reinforcement level, cracking and spelling of concrete due to volume increase of steel reinforcement. Different methods were investigated to overcome corrosion by numerous researchers. A possible solution to combat reinforcement corrosion for new construction is non-corrosive material for replacing steel. Light weight Eminent tensile strength and corrosion less characteristics make Fiber reinforced Polymer (F.R.P) suitable for such applications.

F.R.P in concrete has increased in recent time on account of resistance against corrosion, high tensile strength to weight ratio, and non-magnetization. The supremacy of the F.R.P

How to cite this paper: Prerna Vaidya | Prof. Nitesh Kushwaha | Prof. Afzal Khan "An Analysis of Mechanical Properties and Flexural Behavior of Concrete Slabs Reinforced with H.F.R.P Reinforcements: A Review" Published in International Journal of Trend in Scientific Research and Development (ijtsrd), ISSN: 2456-6470, Volume-5 | Issue-2, February 2021, pp.1200-1212, URL: www.ijtsrd.com/papers/ijtsrd38689.pdf



IJTSRD38689

Copyright © 2021 by author (s) and International Journal of Trend in Scientific Research and Development Journal. This is an Open Access article distributed under the terms of the Creative Commons Attribution License (CC BY 4.0) (<http://creativecommons.org/licenses/by/4.0/>)



materials, in comparison to normal building material such as steel bars, timber and RCC, lies in its improved strength and durability, stability, stiffness.

The main aspect of present research is to review the analytical and experimental behaviour of Hybrid Fiber Reinforced Polymer reinforcements F.R.P (H.F.R.P) reinforcements in concrete one-way slabs on the basis of more accurate modeling and analysis and to build better recommendations for more balanced design. This chapter gives the development, constituents, classification, manufacturing methods and different applications of F.R.P materials. The manufacturing process of new H.F.R.P rod is also explained. Finally it presents need for present study and organization of the thesis.

1.2. TYPES OF FIBERS AND ITS CONSTITUENTS

Fibers are typically Glass F.R.P, Carbon F.R.P, Aramid F.R.P and Basalt F.R.P while the polymer is generally an epoxy, polyester thermosetting plastic. Fibers possess a high strength and high stiffness, toughness and durability. Dimension such as length, cross sectional area, shape & chemical composition plays a main role in imparting good characteristics for fibers along with its corrosion resistant while compare with normal steel reinforcement.

1.3. FIBERS AND PROPERTIES

Fiber properties can differ depending on way of production and bar diameter. Unlike steel, F.R.P continues to exhibit a linear stress-strain correlation upto rupture, without yielding or strain hardening. In F.R.P bar the fiber are the major weight carrying element, therefore the type, ratio and orientation of these fibers play a big responsibility in strength of F.R.P bars. They also determine the rate of curing, the manufacturing process and quality control that is required. Typical properties of different fibers which are report in **ACI 440.1R-15, 2015** shown in the table.

Table 1.1 Typical properties of Various Fibers (ACI 440 1R-15)

Properties	Steel	GF.R.P	C.F.R.P	AF.R.P
Nominal yield stress (MPa)	276 – 517	N/A	N/A	N/A
Tensile strength (MPa)	483 – 690	483 – 1600	600 – 3690	250 -2540
Elastic modulus (GPa)	200	35 – 51	120 – 580	41 – 125
Yield strain %	0.14 – 0.25	N/A	N/A	N/A
Rupture strain %	6.0 – 12.0	1.2 – 3.1	0.5 – 1.7	1.9 – 4.4

Fibers are available in various forms as given in Fig 1.1 to fulfill the requirements. Fibers possess a linear elastic behaviour under tensile loading up to failure without showing yielding. Carbon and aramid fibers are anisotropic with different values of mechanical and thermal properties in the main directions whereas glass fibers are isotropic materials in nature.

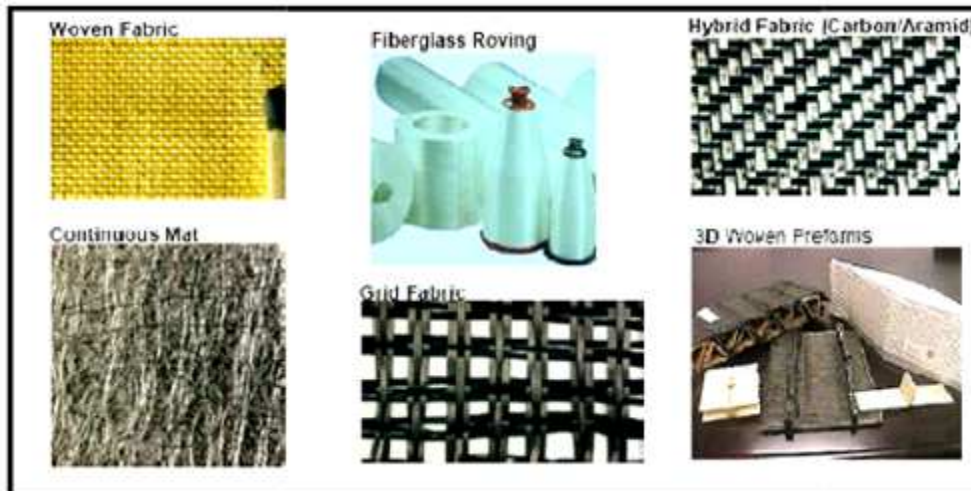
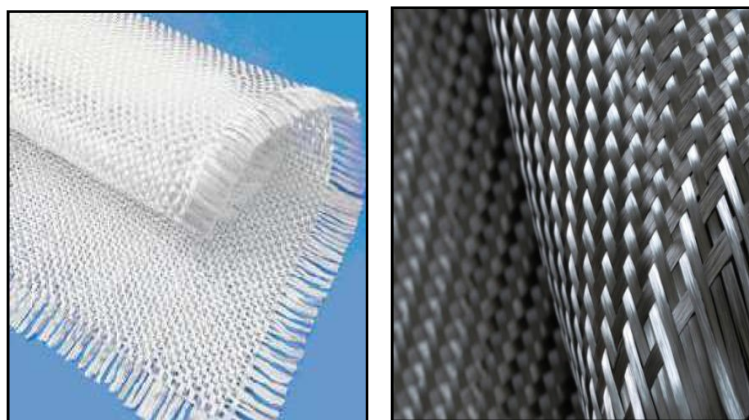


Figure 1.1 Different forms of F.R.P reinforcements (Benjamin 1981)

Glass fibers recommend an economical balance between cost and specific strength properties; this makes them preferable to carbon and aramid in for the most part reinforced concrete (RC) applications. In recent times basalt fibers have emerged as one of the F.R.P materials. Fig.1.2 shows the different rovings of fibers.



Woven Roving GF.R.P

Woven Roving C.F.R.P



(a) Glass rovings (b) Carbon rovings
Fig.1.2 Different rovings of fibers ((Benjamin 1981)

1.4. F.R.P in Structural Engineering

In the last 20 years, compound materials have been built up into inexpensively and structurally feasible building material for buildings and bridges. Fig.1.3 Typical stress-strain in tension for F.R.P bars and steel. Today, F.R.P are new in structural engineering in a variety of forms: reinforcement material for new concrete construction, strengthening material for existing structures, and structural members for new construction. F.R.P material can be used in new construction as internal rebars, prestressing tendons, and stay in-place formwork. The exterior of the F.R.P bars are either sand coated, helically wound spiral outer surface, indented, or with ribs. Figure 1.4 shows some available F.R.P rebar with different surface textures.

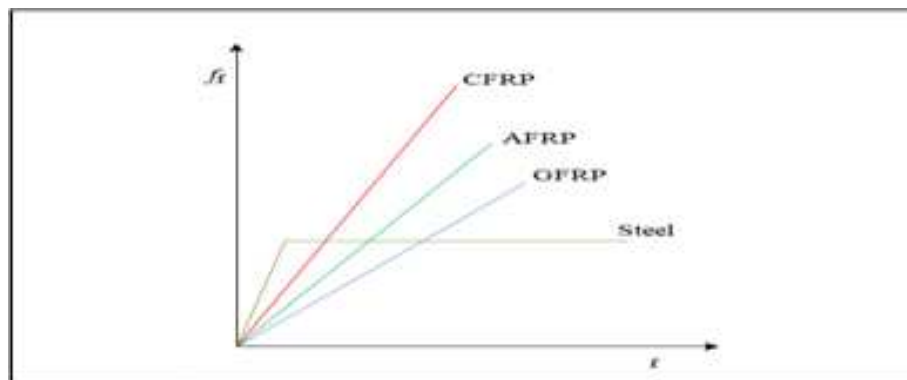


Fig.1.3 Typical stress-strain in tension for types of F.R.P bars and steel

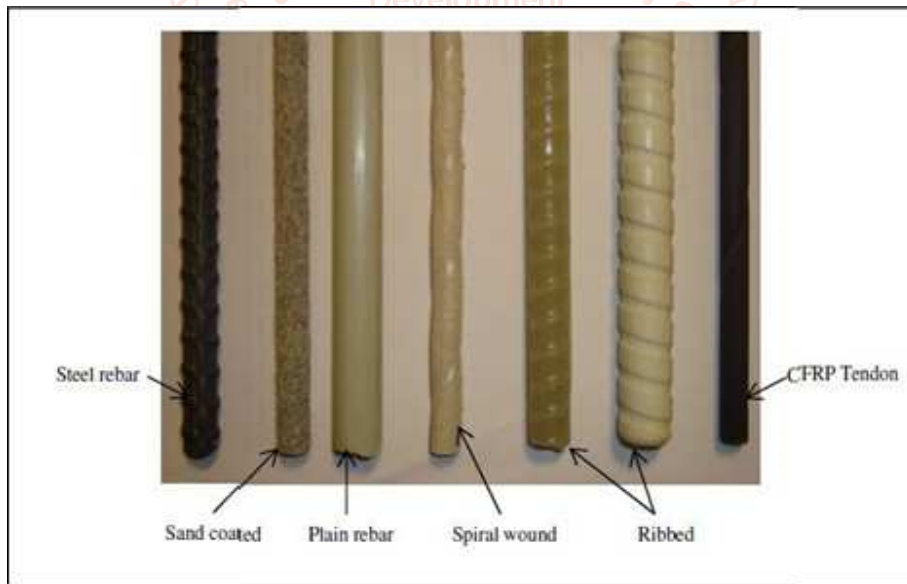


Figure 1.4 Different types of F.R.P rebars available commercially

1.4.1. Glass Fibers

Glass fiber is commercially available in different grade, made from silica sand. The types of glass fibers are electrical (E-glass), high- strength (S-glass), and alkali-resistance (AR-glass). E-glass has high electrical protecting properties, low vulnerability to dampness or moisture, and high mechanical properties. S-glass has higher tensile strength and modulus, in any case, its higher cost make it less best than E-glass. AR-glass is exceedingly impervious resistant to alkali assault in cement- based matrices, however at the development, estimating perfect with thermo set resin that are normally used to pultrude F.R.P bars are not accessible. Composites produced with glass fiber show great electrical and thermal insulation properties.

1.4.2. Carbon Fibers

Carbon fiber is the dominating structure utilized in the structural designing application. Carbon fibre is produced using polyacrylonitrile (PAN), pitch, or rayon fiber precursors PAN based. Polyacrylonitrile carbon fiber shows good strength and

relatively high modulus. Pitch-based carbon fiber has higher modulus yet bring low strength, which makes it appropriate for aviation applications. Fatigue, high resistance to alkali or acid attack, a low C.T.E (Coefficient of thermal expansion), relatively low impact resistance, and high electrical conductivity are high in carbon fiber and it can cause galvanic with metals. In addition, it isn't effortlessly wet by resin; in this manner, sizing is necessary before embedding.

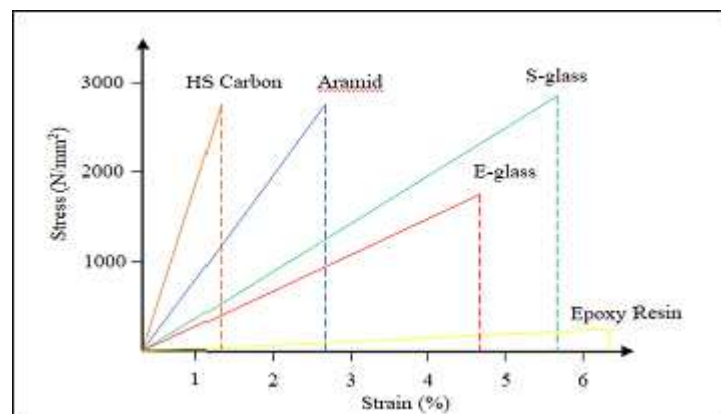


Fig.1.5 Stress-strain relationship to failure for E-glass, S-glass, Aramid, and HS Carbon (Wu, 1990)

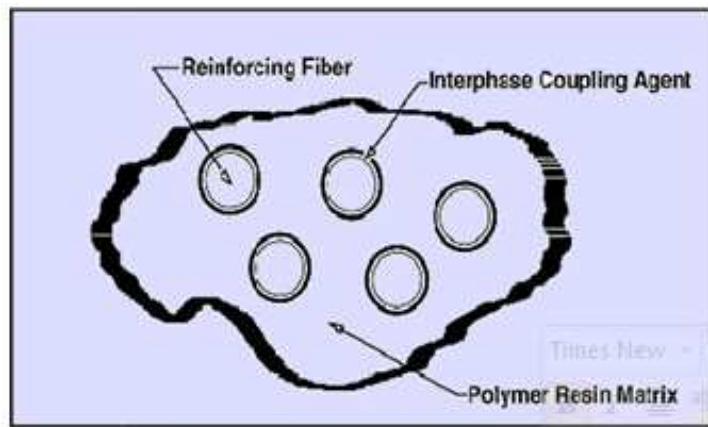


Fig.1.6 Composition of F.R.P material

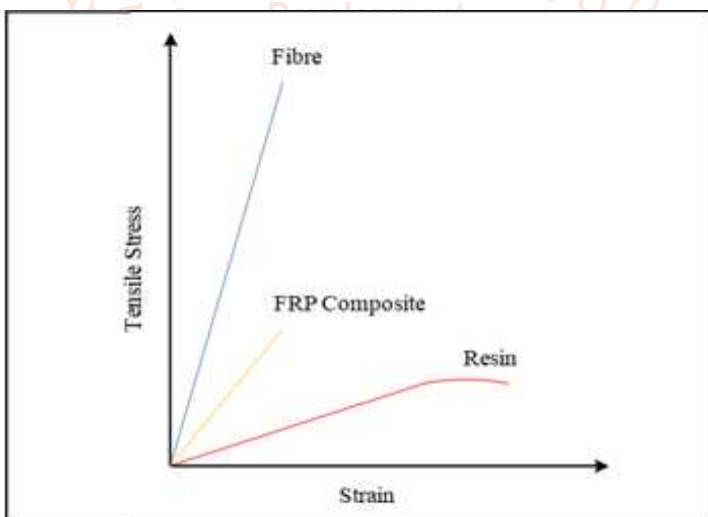


Figure 1.7 Stress-strain relationships for resin, fibers, F.R.P composite

1.5. APPLICATION OF F.R.P REBARS

The common applications are to make use of F.R.P bars to decrease the hazard of corrosion in RCC structures. The life of these types of structure is strictly conditional with the durability of the global reinforcement.

Although their primary cost (raw material and manufacturing costs) and environmental impact (CO_2 production through the manufacturing process) of these kind of bars may be faintly higher than conventional steel, the use of F.R.P bars in concrete structure subjected to insensitive environments generates a significant potential for extending the life of structure and lowering their overall cycle cost and other application of F.R.P rebars are in Ports infrastructure, bridges at sea, retaining/sea walls, and dry docks, Bride decks and railings where deicing salts are used and in Locks and dam weirs. F.R.P bars is also used in the manufacture of equipment which are more receptive to electromagnetic fields.

1.6. ADVANTAGES AND DISADVANTAGES OF F.R.P BARS

Before coming to the usage, any material should be thoroughly analysed for its good and poor sides. Table 1.2 shows the merit and demerits of F.R.P material when used in the form of rebars in concrete.

Table 1.2 Shows the advantages and disadvantages of F.R.P material

Advantages	Disadvantages
F.R.P bars is more durable and diversified in its applications	No yielding before brittle rupture
It is more durable and cost effective than steel	Design components made from F.R.P is complex.
Less maintenance and the cost is lower or nil	Manufacturing and testing of F.R.P components is highly specialized.
Low transportation and installation costs.	Poor rigidity and stiffness.
Withstanding chemical attacks and moisture proves non-fatal, unlike steel.	Application is limited to a temperature below 300-degree Celsius.
Lightweight material and help contractors to deliver projects at a fast pace	May be susceptible to fire depending on matrix type and concrete cover thickness.

2. REVIEW OF LITERATURES

2.1. GENERAL

This Chapter contains a detailed survey of literature that provides the previous work. The initial part of this chapter covers the review on properties of F.R.P along with durability aspects. Second part covers a assess the bond performance of the F.R.P and concrete. The third section short review of literature concerned on the flexural behavior of F.R.P structural components. Fourth section covers the analytical modelling for the examination of F.R.P reinforced structural components.

Hongseob oh et al., (2019) carried out the bond test on G.F.R.P beams subjected under two point monotonic loading condition. The results stated that G.F.R.P rebar possess good mechanical interlocking with concrete conventional ones. It is understood that pullout test, tensile test overestimates the bond capacity of beams. According to the findings, it concluded that G.F.R.P rebar had a the bond slip values when compared to steel rebar.

Qasim and Hayder (2018) ANSYS yields good agreement with experimental results for both types of slabs rather than numerous values obtained by adopting equations of **ACI 440.1R-15, 2015.**

Travares et al., (2018) compared the strength, deformation of fine G.F.R.P beams with one conventional beam. To get the actual flexural response of G.F.R.P beams, it control the stiffness and the internal tension force. This study has also forced to design the G.F.R.P beams based on serviceability and ultimate limit-state.

Arindom bora et al., (2018) has carried out design beam column joint reinforced with four types of F.R.P (G.F.R.P, C.F.R.P , BF.R.P and AF.R.P) reinforcements . Results it is noted reduced equivalent stress on the introduction of F.R.P. The ultimate equivalent stress occurred and the beams of the beam column joint. Total deformation column joint are satisfactory.

Arabshahi (2017) studied to assess precision for F.R.P bars are under available relations to computation of in concrete beams. Branson relation is used and modified in concrete members. Different reliability indexes are evaluated in concurrence with different technique. from different studies available relations. Based on this investigation, the most accurate and reliable relations are identified. Furthermore, a new relation based on numerical methods will be proposed.

Premalatha et al., (2017) has created G.F.R.P and conventional RC beams, using ANSYS 16.2.the results

(ultimate load and cracking behaviour) very closer to value and showing 10% variation. All the beams are failed ultimate stage.

Krishnan et al., (2017) analysed of square columns using ANSYS. columns confined by G.F.R.P sheets showed better results than column confined by C.F.R.P sheets and unconfined RC columns. The G.F.R.P and C.F.R.P confinement enhanced the RC columns. concluded that ANSYS worked well for predicting F.R.P confinement of nonlinear behaviour of RC columns.

Xingyu Gu et al., (2016) studied the G.F.R.P and considering three test specimens. geometric size of both G.F.R.P and steel rebar specimens which have the same bearing capacities. Regarding so many authors have been put forward their opinion through lot of experiments

Triantafillou and Antonopoulos (2016) studied the beam sections with lesser C.F.R.P tensile rupture, layer of C.F.R.P reinforcement. C.F.R.P material which implies experience a abrupt tensile rupture instead of a gradual yielding, as in the case with steel reinforcement.

Vijay and Gangarao (2016) compiled and overcome a list tests and analysed them to understand how the flexural capacity openly relates to properties of the reinforcing bars. They identified that, the preferred failure mode of G.F.R.P RC in flexure is concrete crushing because the compression induced failure provides better deformability at ultimate conditions and it has less deflection and crack widths at service load levels. While the benefit of better deformability is true because of the nature of compression failure, reduced cracks and deformation at service loads is primarily the effect of over-reinforcing with G.F.R.P bars, something that is necessary to ensure compression failure.

Issa et al., (2016) observed that good features over steel by their high strength, stiffness/weight ratios and durability against corrosion and chemicals and finally thermal properties when compared with structural members reinforced with conventional bars.

Al-Sunna et al., (2015) experimentally investigated the deflection behaviour of 24 G.F.R.P and C.F.R.P slabs' covering varies of reinforcement ratios. From this investigation, it is indicated that further deformations tempted by pure flexure might be important mainly in F.R.P with reasonable to high reinforced ratio. Though, it seems that simplified methods to predict deflections of F.R.P RC elements take into explanation from these additional deformations. This un-conservative predictions particularly.

SUMMARY

This chapter has presented the review of literature of basic properties of F.R.P reinforcements, behaviour of F.R.P reinforced concrete flexural members, numerical modelling and analysis under strength and serviceability requirements of F.R.P reinforced concrete flexural components and on reliability study on the F.R.P reinforcements. Objectives, Scope and Methodology of the present work are defined.

3. PROBLEM IDENTIFICATIONS AND OBJECTIVES

3.1. Problem Identifications

This has been seen that no detail study has been done on the utilization of more than one fiber in one member of the structure. Concept of hybrid fibers is well known to us, and its utilization is effective in terms of modifying mechanical properties. It has been observed in previous literatures that there is lots of scope in utilization of hybrid fibers in concrete members.

3.2. Objectives

- To study different mechanical properties of steel, HFRP reinforcements and concrete like density, tensile strength, thermal expansion coefficient, modulus of elasticity.
- To analyze the flexural behavior of HFRP reinforcements in concrete slabs with steel reinforcements.
- To study the flexural behaviour of concrete slabs reinforced with HFRP and conventional reinforcements under two point static loading conditions.
- To propose modified theoretical expressions for the flexural capacity, deflections and crack widths for the HFRP reinforced concrete one-way slabs under two point static loading conditions.

4. METHODOLOGY

4.1. GENERAL

In this chapter laboratory tests carried out to evaluate the mechanical and physical properties of the newly developed H.F.R.P bars and have a comparison with that of conventional bars.

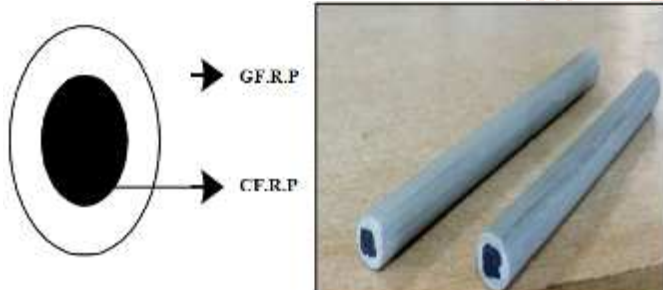


Figure 4.1 Cross Section View of H.F.R.P Bar

4.2. MECHANICAL AND PHYSICAL PROPERTIES OF H.F.R.P BARS

In this section, properties which are consider to be important to know about the H.F.R.P bars and to interact with concrete have been determined in materials laboratory.

4.2.1. Density

According to A.S.T.M D792-13 standards the density of H.F.R.P bars have been evaluated the experimental value with 0.1mg precision. As per the standards, the H.F.R.P bars are weighed. Then, the H.F.R.P bar is immersed in distilled water at 230C and the wet weight of the bar is noted. The weight of the sinker in immersed condition is also noted. The specific gravity is calculated by using the Eq. 3.1 and Eq. 3.2. Table 3.1

presents the density of bars indicated in (ACI440. IR-15,2015).

$$\text{Specific gravity } (23^{\circ}\text{C}) = a / (a + w - b) \quad (\text{Eqn 3.1})$$

$$\text{Density } (23^{\circ}\text{C}) = \text{specific gravity } 23^{\circ}\text{C} \times 997.5 \text{ Kg/m}^3 \quad (\text{Eqn 3.2})$$

A - Apparent mass of specimen, before immersion in water sinker,

B - Apparent mass of the specimen and the sinker immersed in water,

w - Apparent mass of the immersed.



Figure 4.2 Density Test Setup Of H.F.R.P Bars

4.2.2. Tensile test

According to **ASTM D7205/D7205M-06(2011)** the specimens are prepared for the tensile test. Total length of specimen is 1000mm and length is 400mm. Two 300mm long steel tube anchor with an outside diameter of 25.4 mm and thickness of 3mm is used at both ends of sample for gripping. Steel Plugs and PVC caps drilled on their centre slightly bigger than the bar diameter are used to close on both the ends of steel tube ad to insert the specimens at the centre of the steel tube. Fig 4.3 shows the steel tube used for gripping position of H.F.R.P bars and Figure4.4 shows the details of the tensile test specimens. Then the gap between the steel tubes filled with mixture of epoxy resin and hardener and allowed for 24 hours curing. The specimen is cured for 7 days in typical indoor laboratory conditions.



Figure 4.3 Steel tube used for gripping position of H.F.R.P bars

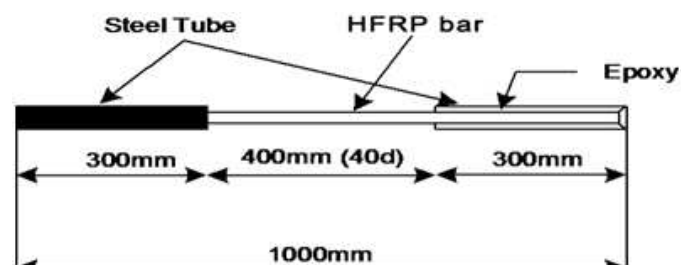


Figure 4.4 Details of tensile test specimens

This test has been conducted at Strength of materials laboratory, Department of Structural engineering.



Figure 4.5 Tensile test setup

Stress-strain curve

The stress-strain response of the sand-coated H.F.R.P bars is linear, does not have any yield point up to the failure. The failure stress could be much more than the conventional steel bar. The change in size of the H.F.R.P bars does not make any change in stress strain response. The strain and stress response of conventional steel bars beyond the elastic portion, yielding occurs at beginning of plastic deformation.

4.2.3. TRANSVERSE SHEAR STRENGTH

Transverse shear strength is conducted to measure shear strength of HFRP bars by using **ASTM D7617/D7617M** describes method of sampling, fixturing, testing composite reinforcing bars and conditioning and smooth round reinforcements in transverse shear. As per **ASTM D 7617**, size of reinforcements is cut and transverse shear test has carried out on HFRP and steel and compared.

The displacement rate is selected as 1.84mm/min so that the test specimens fail at a time between 1 and 3 minutes. By applying the load, the bar shears at two places and the ultimate load has been noted.



(a) Transverse shear test setup



(b) Shear failure of specimen

Figure 4.6 Transverse shear test

4.2.4. COEFFICIENT OF LINEAR THERMAL EXPANSION

The Coefficient of linear thermal expansion (α) is calculated using this formula Eq. 3.7

$$\alpha = \Delta L / L_0 \Delta T \quad (\text{Eqn.3.7})$$

Where ΔL is the change in length of the specimen, L_0 is the original length of the specimen, ΔT is the temperature change during the test.



Figure 4.7 Dilatometer test setup

4.2.5. BOND MECHANISM

The bonding of concrete with reinforcing bars is the key to develop composite action of RC elements. The properties of F.R.P bars are dissimilar to steel bars. At service loads, the tension stiffening effect of the concrete is affected by the F.R.P bars due to its difference local bond behavior which turn affects the cracking and deflection of RC member. Therefore, the bond test also has been carried out in the present study.

The tensile strength and elastic modulus of H.F.R.P bars were calculated and tested according to **ASTM D7205/D7205M06**. The tensile properties of H.F.R.P and steel bars were listed in Table 4.1. The mix ratio of cement water fine aggregate coarse aggregate-super plasticizer is 1:0.38: 1.56: 2.72: 0.005. The maximum size of coarse aggregate is 20mm and the fine aggregate is river sand with a particle size of 0-5mm. The specific gravity of fine aggregate and coarse aggregate is 2.63 and 2.72 respectively. The average compressive strength of concrete at 28 days is arrived at 49 MPa. The concrete cubes for pullout specimens consisted of, 200mm on each edge, with a single 1200mm long H.F.R.P bar embedded vertically along the central axis in each specimen Figure 4.9 to 4.10 shows the preparation of specimens. The embedded length of the H.F.R.P bar was five times the diameter of the H.F.R.P bar.

The embedded bar inserted within (PVC) pipe to prevent bonding at top of each specimen, and additionally, the PVC pipe is used to avoid splitting of concrete during the pull-out test. Steel tubes are used as anchors at the loaded end of the H.F.R.P bars and are cast with epoxy resin and hardener. The pullout specimens are cast in accordance with C192/C192M. Then, the moulds are removed from the specimens after 20 hours of casting. After removing the moulds, the specimens are cured until the time of testing and the pullout specimens were tested after the period of 28 days. Tensile properties of H.F.R.P and Steel bars are shown in Table 4.1.

Table 4.1 Tensile Properties of H.F.R.P And Steel Bars

Specimen	Bar Diameter (mm)	Cross sectional area (mm ²)	Surface characteristics	Tensile strength (MPa)	Elastic modulus (GPa)
HF.R.P	10	78.5	Sand-coated	1217.93	50.5
STEEL	10	78.5	Deformed	591.3	200

**Figure 4.9 Wooden Mould****Figure 4.10 PVC tube****Figure 4.11 Anchor as per ASTM D7205****Figure 4.12 Arrangements of H.F.R.P bars (ready for casting) and casting on concrete cube**

4.2.6. Pull Out Test Setup

The bond strength of the H.F.R.P bar is assessed by testing five samples as per **ASTM D7913/D7913M-14**. This pullout test is conducted at Universal Testing Machine (UTM). The steel tube anchorages are provided as a shield to avoid crushing of the H.F.R.P bar at its ends. This steel tube is fixed by conventional wedge frictional grip at machine's lower jaw. The pullout is performed by pulling the steel tube toward one side. Fig.4.13 demonstrates the test setup for pullout test. Fig.4.14 shows one linear variable differential transformer (LVDT) which is fitted to the top extended free end of the H.F.R.P bar at outside of the concrete cube and then load is applied gradually at a rate of 20kN/min up to failure of the specimen. The pullout load and displacement (slip) values are recorded during the test by a computer controlled acquisition system.

**Figure 4.13 Pullout Test Setup****Figure 4.14 LVDT at free end of H.F.R.P**

Eqn.3.8 shows the calculation of bond stress with the data collected from experiment

$$v = \frac{F}{c_b S} \dots \dots \dots \text{Eqn.3.8}$$

Where τ is the average bond stress (MPa), F is the tensile force (N), C_b is the circumference of F.R.P bar, and l is the bonded length (mm). The slip of the H.F.R.P bars in concrete can be achieved and showed on Eqn.3.9.

$$s = s_L - s_F$$

(Eqn.3.9)

Where s is the slip of the H.F.R.P bars (mm); s_L is the loaded end slip of the H.F.R.P bar (mm); s_F is the free end slip of the H.F.R.P bars (mm).

4.3. MATERIAL PROPERTIES

4.3.1. Concrete

Normal Strength Concrete (NSC) of grades 30MPa, 40MPa and 50MPa are used to cast the concrete one-way slabs. Ordinary Portland Cement (OPC), coarse aggregate size of 20mm and fine aggregate of size ranging up to 4.75mm sieve are used in casting the slabs and in real environmental conditions. After 28 days of curing the compressive strength of cubes are determined with 150mm size of standard test cubes using Compression testing machine and the properties of concrete are tabulated in Table 4.2.

Table 4.2 Properties of Concrete

Material	M30 grade of concrete	M40 grade of concrete	M50 grade of concrete
Cement, kg/m ³	425.34	430	450
Fine aggregate, kg/m ³	615.21	664	701
Coarse aggregate, kg/m ³	1181.52	1174	1163
Water, kg/m ³	191.58	165	160
Average compressive strength, N/mm ²	38	49	56

4.3.2. Reinforcements

The properties of reinforcements are already explained which results are further explain in next chapter.

Table 4.3 Properties of Reinforcements used in the study

Properties	Type of Rebar	HF.R.P	STEEL
Tensile Strength, MPa	1217.93	583.67	
Compressive strength, MPa	746.17	435.68	
Elastic modulus, GPa	50	200	
Transverse Shear strength, MPa	418.4	302.5	
Coefficient of linear expansion, /° C	9x10 ⁻⁶	20 x10 ⁻⁶	

4.4. TEST SPECIMEN PREPARATION

The experimental program consists of eighteen one-way slabs of length 2400mm and 600mm width. The various parameters that are involved in the present study and their designations are tabulated in Table 4.4. The reinforcements of size 8 mm are used as secondary reinforcements in the transverse direction of slab i.e. widthwise and 10 mm reinforcements are used as main reinforcements in the span direction of slab i.e. lengthwise at three different spacing viz., 186.6 mm c/c, 140 mm c/c and 93 mm c/c. Main and secondary H.F.R.P reinforcements are tied with help of Nylon zip ties.

4.5. TEST SPECIMEN PREPARATION

The experimental program consists of eighteen one-way slabs of length 2400mm and 600mm width. The various parameters that are involved in the present study and their designations are tabulated in Table 4.4. The reinforcements of size 8 mm are used as secondary reinforcements in the transverse direction of slab i.e. widthwise and 10 mm reinforcements are used as main reinforcements in the span direction of slab i.e. lengthwise at three different spacing viz., 186.6 mm c/c, 140 mm c/c and 93 mm c/c. Main and secondary H.F.R.P reinforcements are tied with help of Nylon zip ties. Secondary (8mm steel/H.F.R.P) reinforcements are spaced at 210 mm c/c. Main reinforcements are given a bottom cover of 20mm for all the slabs. Mixing of concrete is done with help of rotary mixers. The slabs are designated with the parameters of m1hp1D1, m1hp2D1, m1hp3D1, m2hp1D1, m2hp2D1, m2hp3D1, m1hp1D2, m2hp1D2, m3hp1D2, m1sp1D1, m1sp2D1, m1sp3D1, m2sp1D1, m2sp2D1, m2sp3D1, m1sp1D2, m2sp1D2, m3sp1D2. Normal moist curing is done for all slabs; After curing, grid points are marked to locate the loading points and strain measuring positions; Brass pellets are fixed to measure strains using Demouldable mechanical (Demec) strain gauge. In the next section a detailed experimental setup is explained under different loading conditions

Table 4.4 Various Parameters involved in the construction of slabs

Parameters	Description	Designation
Types of reinforcements	H.F.R.P	h
	Steel	s
Thickness of slabs	100 mm	D_1
	120 mm	D_2
Grades of concrete	M30	m_1
	M40	m_2
	M50	m_3
Reinforcement ratios	0.49%	hp_1, sp_1
	0.65%	hp_2, sp_2
	0.81%	hp_3, sp_3

4.6. TEST SETUP AND INSTRUMENTATION

Load frame of capacity 50 tonnes is used for testing the slab specimens. Slabs are supported with following end condition; i.e. one end of the slab rests on roller support and the other end rests on hinge support. Two point loading (line loads) system is used with the help of spreader beams. Thick rubber or neoprene pads are kept under the spreader beams to avoid local effects. The support end levels of the slabs were maintained properly by spirit levels. The static loads are applied with the help of hydraulic jacks manually (250 kN capacity) and are monitored by proving ring or load cells. The deflections or deformations of the slab are measured by dial gauges and Demec gauges. All slabs are pasted with internal and external surface strain gauges. Internal strain gauges are glued on the surface of the steel/H.F.R.P reinforcements at the time of casting the slabs with due precaution. External strain gauges are fixed on the surface of the slabs at top and bottom fibers. Dial gauges are also fixed at centre, one-third load points and at supports. Dial gauges are fixed at the supports to carry out support corrections. Demec gauges are also used at centre and one-third load points to measure the linear strains. To measure strains with help of Demec gauges, a standard gauge distance is required and it is done with the help of brass pellets pasted at a known distance at top, bottom and centre fibers. A hydraulic jack with the capacity of 250KN is used to apply the load statically on the slabs and the application of load is controlled by proving ring. The experimental set up is shown in Figure 4.14, test setup for static loading shown in Fig 4.15 and finally, Fig 4.16 shows the test setup for static loading under loading condition respectively. The static load is gradually applied approximately with an increment of 2 kN up to the failure of the slabs. The corresponding deflections are noted. The crack widths are measured periodically by using crack width detection microscope.

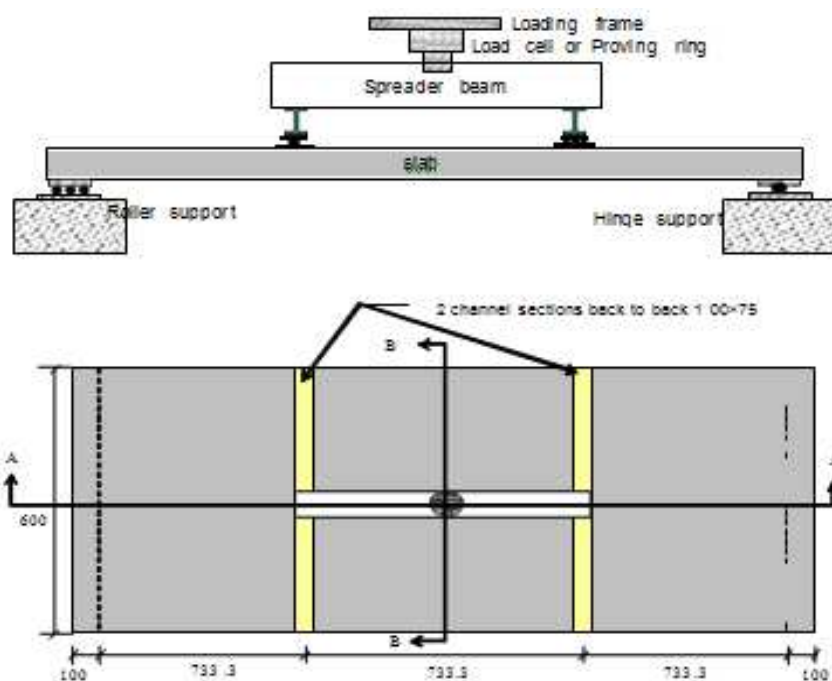


Figure 4.14 Experimental Test setup

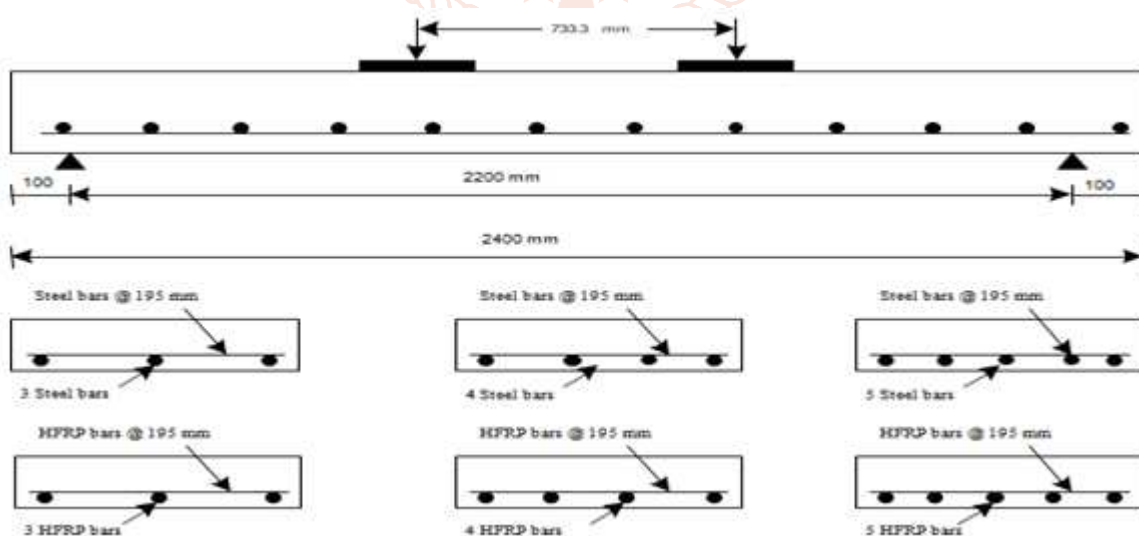


Figure 4.15 Reinforcements Details for H.F.R.P And Conventional Slabs



Figure 4.16 Test Set Up For Static Loading



Figure 4.17 Test set up for Static loading under loading condition

4.7. DEFORMABILITY FACTORS

Ductility is the energy absorption capacity of a structure without failure and is to measure the inelastic deformation. For steel-reinforced structures, ductility is the ratio between the ultimate deformation and the deformation at yielding. This way of estimating ductility cannot be applied to F.R.P reinforced structures because they are virtually linear until failure.

Deformability factors quantify the safety of a H.F.R.P-reinforced member similar to ductility factors in numerically. This factor, however, does not incorporate the advantageous post-yield behaviour of steel-reinforced flexural members. According to, a large curvature is needed for a higher moment of resistance. Thus, an accurate quantification of safety must account for load resistances (moments, forces, or stresses) as well as member deformations (curvature, displacement, or strains).

Deformability factors overcome this problem. A flexural member, properly designed with adequate deformability, can meet serviceability requirements, but still have enough reserve strength and deflection to allow pre-emptive warning of failure. Deformability factors account for this effect by comparing energy absorption at two different load levels i.e. energy absorbed at ultimate state with the energy absorbed at service load level. For the present study DF has been calculated from the experimental observations.

The Deformability Factor DF shown in Eqn 3.13 is obtained by multiplying the Moment factor by Curvature factor; accordingly,

$$DF = \text{Moment factor} \times \text{Curvature factor}$$

i.e., MF = Moment factor = $\frac{(M_u)}{(M_s)}$ and CF= Curvature factor $\frac{(\Psi_u)}{(\Psi_s)}$

Therefore, DF = $\frac{(M_u)}{(M_s)} \times \frac{(\Psi_u)}{(\Psi_s)}$ (3.13)

By the use of deformability factor, the ratio of Mu at ultimate and service load conditions are used as a practical means to indicate approximately the ratio of the strain energy values at the two load levels.

The procedure is based on restriction of cracks widths at service load condition and ensuring that adequate deformability of the slab occurs before failure. By limiting the stress in the reinforcements it can be achieved. The stress in H.F.R.P reinforcements at service loads is depends on the ultimate strength of slab. Therefore the design requirement governs the amount of H.F.R.P reinforcement ratio provided. Based on this study, the deformability factor exceeds a value of 4 as specified in previous studies (**CEB-FIP, 2007; ACI 440. 1R-15, 2015**). This study limits the strain in H.F.R.P ($\epsilon_{H.F.R.P}$) due to service loads to 1.5 times the strain allowed for steel reinforcements (ϵ_y) which is equal to the strain 0.002 of slab.

Since F.R.P bars do not yield, a deformability factor is used and a minimum required value, DF=4, is proposed. The permissible value of strain in steel is limited to 0.002 as serviceability condition which is proposed to result in crack widths 5/3 times larger than the widths when steel bars are used. It is shown, by a parametric study, that when the F.R.P is determined in this way, the DF is commonly greater than 4; thus, there is no need to check the deformability.

Conclusion

In this Chapter firstly, the manufacturing process of newly developed H.F.R.P bars are presented and secondly, the important properties such as Density, Tensile strength, Transverse shear, Coefficient of Thermal Expansion, and are determined according to ASTM standards and compared with that of conventional bars. The results shows good and satisfactory performance of H.F.R.P bars in comparison with Conventional bars. The bond performance of H.F.R.P rebars with concrete has also been examined. A detailed experimental procedure has been conducted to investigate the flexural behaviour of one-way slabs with all parametric conditions are presented.

REFERENCES

- [1] ACI 544.3R-93: Guide for Specifying, Proportioning, Mixing, Placing, and Finishing Steel Fiber Reinforced Concrete, American Concrete Institute, 1998
- [2] ASTM C1116/C1116M – 06
- [3] "AROVEX™ Nanotube Enhanced Epoxy Resin Carbon Fiber Prepreg – Material Safety Data Sheet" (PDF). Zyvex Performance Materials. 8 April 2009. Archived from the original (PDF) on 16 October 2012. Retrieved 26 March 2015.
- [4] ACI-318-IBC-IRC-Evaluation-report-Helix-Steel-Micro-Rebar-Alternative-to-Steel-Rebar-Concrete-reinforcement-Vertical-Applications.pdf
- [5] Almudaihesh, Faisel; Holford, Karen; Pullin, Rhys; Eaton, Mark (1 February 2020). "The influence of water absorption on unidirectional and 2D woven CFRP composites and their mechanical performance". Composites Part B: Engineering. **182**: 107626. doi:10.1016/j.compositesb.2019.107626. ISSN 1359-8368.
- [6] "AERO – Boeing 787 from the Ground Up". Boeing. 2006. Archived from the original on 21 February 2015. Retrieved 7 February 2015
- [7] "Busted Carbon". Archived from the original on 30 November 2016. Retrieved 30 November 2016.
- [8] "Carbon Technology". Look Cycle. Archived from the original on 30 November 2016. Retrieved 30 November 2016.
- [9] "Carbon fibre reinforced plastic bogies on test". Railway Gazette. 7 August 2016. Archived from the original on 8 August 2016. Retrieved 9 August 2016.
- [10] Corum, J. M.; Battiste, R. L.; Liu, K. C; Ruggles, M. B. (February 2000). "Basic Properties of Reference Crossply Carbon-Fiber Composite, ORNL/TM-2000/29, Pub57518" (PDF). Oak Ridge National Laboratory. Archived (PDF) from the original on 27 December 2016.
- [11] "Engines". Flight International. 26 September 1968. Archived from the original on 14 August 2014.
- [12] FIRE PROTECTION OF CONCRETE TUNNEL LININGS by Peter Shuttle worth, Rail Link Engineering. UK
- [13] Guzman, Enrique; Cugnoni, Joël; Gmür, Thomas (May 2014). "Multi-factorial models of a carbon fibre/epoxy composite subjected to accelerated environmental ageing". Composite Structures. **111**: 179–192. doi:10.1016/j.compstruct.2013.12.028
- [14] Guzman, Enrique; Gmür, Thomas (dir.) (2014). "A Novel Structural Health Monitoring Method for Full-Scale CFRP Structures" (PDF). EPFL PhD thesis. doi:10.5075/epfl-thesis-6422. Archived (PDF) from the original on 25 June 2016.
- [15] Henry, Alan (1999). McLaren: Formula 1 Racing Team. Haynes. ISBN 1-85960-425-0.
- [16] Howard, Bill (30 July 2013). "BMW i3: Cheap, mass-produced carbon fiber cars finally come of age". Extreme Tech. Archived from the original on 31 July 2015. Retrieved 31 July 2015.
- [17] Hans, Kreis (2 July 2014). "Carbon woven fabrics". compositesplaza.com. Archived from the original on 2 July 2018. Retrieved 2 January 2018.
- [18] "How is it Made". Zoltek. Archived from the original on 19 March 2015. Retrieved 26 March 2015.

[19] "ICC and Kookaburra Agree to Withdrawal of Carbon Bat". NetComposites. 19 February 2006. Retrieved 1 October 2018.

[20] Ismail, N. "Strengthening of bridges using CFRP composites." *najif.net*.

[21] *Jump up to:^a ^b ^c* Courtney, Thomas (2000). *Mechanical Behavior of Materials*. United States of America: Waveland Press, Inc. pp. 247–249. ISBN 1-57766-425-6.

[22] *Jump up to:^a ^b ^c ^d ^e ^f* Chawla, Krishan (2013). *Composite Materials*. United States of America: Springer. ISBN 978-0-387-74364-6.

[23] Kopeliovich, Dmitri. "Carbon Fiber Reinforced Polymer Composites". Archived from the original on 14 May 2012.. *substech.com*

[24] Li, V.; Yang, E.; Li, M. (28 January 2008), *Field Demonstration of Durable Link Slabs for Jointless Bridge Decks Based on Strain-Hardening Cementitious Composites – Phase 3: Shrinkage Control (PDF)*, Michigan Department of Transportation

[25] LaChance, David (April 2007). "Reinventing the Wheel Leave it to Citroën to bring the world's first resin wheels to market". *Hemmings*. Archived from the original on 6 September 2015. Retrieved 14 October 2015.

[26] Lomov, Stepan V.; Gorbatikh, Larissa; Kotanjac, Željko; Koissin, Vitaly; Houle, Matthieu; Rochez, Olivier; Karahan, Mehmet; Mezzo, Luca; Verpoest, Ignas (February 2011). "Compressibility of carbon woven fabrics with carbon nanotubes/nanofibres grown on the fibres". *Composites Science and Technology*. **71** (3): 315–325. doi:10.1016/j.compscitech.2010.11.024.

[27] *Mechanical Properties of Recycled PET Fibers in Concrete, Materials Research*. 2012; **15**(4): 679–686

[28] "News - Fibres add much needed protection to prestigious tunnelling projects". 2007-09-27. Archived from the original on 2007-09-27. Retrieved 2017-02-05.

[29] Nguyen, Dinh; Abdullah, Mohammad Sayem Bin; Khawarizmi, Ryan; Kim, Dave; Kwon, Patrick (2020). "The effect of fiber orientation on tool wear in edge-trimming of carbon fiber reinforced plastics (CFRP) laminates". *Wear*. Elsevier B.V. 450–451: 203213. doi:10.1016/j.wear.2020.203213. ISSN 0043-1648.

[30] Ochiai, T.; Okubob, S.; Fukuib, K. (July 2007). "Development of recycled PET fiber and its application as concrete-reinforcing fiber". *Cement and Concrete Composites*. **29** (6): 448–455. doi:10.1016/j.cemconcomp.2007.02.002.

[31] Pora, Jérôme (2001). "Composite Materials in the Airbus A380 – From History to Future" (PDF). *Airbus*. Archived (PDF) from the original on 6 February 2015. Retrieved 7 February 2015.

[32] Pike, Carolyn M.; Grabner, Chad P.; Harkins, Amy B. (4 May 2009). "Fabrication of Amperometric Electrodes". *Journal of Visualized Experiments* (27). doi:10.3791/1040. PMC 2762914. PMID 19415069.

[33] Petrány, Máté (17 March 2014). "Michelin Made Carbon Fiber Wheels For Citroën Back In 1971". *Jalopnik*. Archived from the original on 18 May 2015. Retrieved 31 July 2015.

[34] "Polyamid CF Filament - 3D Druck mit EVO-tech 3D Druckern" [Polyamide CF Filament - 3D printing with EVO-tech 3D printers] (in German). Austria: EVO-tech. Retrieved 4 June 2019.

[35] Pozegic, T. R.; Jayawardena, K. D. G. I.; Chen, J-S.; Anguita, J. V.; Ballocchi, P.; Stolojan, V.; Silva, S. R. P.; Hamerton, I. (1 November 2016). "Development of sizing-free multi-functional carbon fibre nanocomposites". *Composites Part A: Applied Science and Manufacturing*. **90**: 306–319. doi:10.1016/j.compositesa.2016.07.012. ISSN 1359-835X.

[36] "Red Bull's How To Make An F1 Car Series Explains Carbon Fiber Use". *motorauthority*. Archived from the original on 29 September 2013. Retrieved 11 October 2013.

[37] Rahman, S. (November 2008). "Don't Stress Over Prestressed Concrete Cylinder Pipe Failures". *Opflow Magazine*. **34** (11): 10–15. doi:10.1002/j.1551-8701.2008.tb02004.x. Archived from the original on 2 April 2015.

[38] Ray, B. C. (1 June 2006). "Temperature effect during humid ageing on interfaces of glass and carbon fibers reinforced epoxy composites". *Journal of Colloid and Interface Science*. **298** (1): 111–117. Bibcode:2006JCIS..298..111R. doi:10.1016/j.jcis.2005.12.023. PMID 16386268.

[39] Scott, Alwyn (25 July 2015). "Boeing looks at pricey titanium in bid to stem 787 losses". www.stltoday.com. *Reuters*. Archived from the original on 17 November 2017. Retrieved 25 July 2015.

[40] "Taking the lead: A350XWB presentation" (PDF). *EADS*. December 2006. Archived from the original on 27 March 2009.

[41] "The Perils of Progress". *Bicycling Magazine*. 16 January 2012. Archived from the original on 23 January 2013. Retrieved 16 February 2013.

[42] Thomas, Daniel J. (1 September 2020). "Developing hybrid carbon nanotube- and graphene-enhanced nanocomposite resins for the space launch system". *The International Journal of Advanced Manufacturing Technology*. **110** (7): 2249–2255. doi:10.1007/s00170-020-06038-7. ISSN 1433-3015.

[43] Trimble, Stephen (26 May 2011). "Lockheed Martin reveals F-35 to feature nanocomposite structures". *Flight International*. Archived from the original on 30 May 2011. Retrieved 26 March 2015.

[44] "Zyvex Performance Materials Launch Line of Nano-Enhanced Adhesives that Add Strength, Cut Costs" (PDF) (Press release). *Zyvex Performance Materials*. 9 October 2009. Archived from the original (PDF) on 16 October 2012. Retrieved 26 March 2015.

[45] Zhao, Z.; Gou, J. (2009). "Improved fire retardancy of thermoset composites modified with carbon nanofibers". *Sci. Technol. Adv. Mater.* **10** (1): 015005. Bibcode:2009STAdM..10a5005Z. doi:10.1088/1468-6996/10/1/015005. PMID 2109595. PMC 27877268.